

UNCLASSIFIED



AD NUMBER

AD-B007 377

NEW LIMITATION CHANGE

TO

DISTRIBUTION STATEMENT: A

Approved for public release; Distribution is unlimited.

LIMITATION CODE: 1

FROM

DISTRIBUTION STATEMENT: B

LIMITATION CODE: 3

AUTHORITY

USAARDC ltr; Jul 31, 1979

THIS PAGE IS UNCLASSIFIED

✓

✓

BRL MR 2509

BRL

2

AD

MEMORANDUM REPORT NO. 2509 ✓

AD B 007377

CALCULATIONS OF FRAGMENT VELOCITIES
FROM NATURALLY FRAGMENTING MUNITIONS

R. R. Karpp
W. W. Predebon

July 1975

AD No. —
DDC FILE COPY

Distribution limited to US Government agencies only; Test and Evaluation; July 75 Other requests for this document must be referred to Director, USA Ballistic Research Laboratories, ATTN: AMXBR-SS, Aberdeen Proving Ground, Maryland 21005.

USA BALLISTIC RESEARCH LABORATORIES
ABERDEEN PROVING GROUND, MARYLAND

DDC
RECEIVED
NOV 6 1975

19990407163

Destroy this report when it is no longer needed.
Do not return it to the originator.

Secondary distribution of this report by originating
or sponsoring activity is prohibited.

Additional copies of this report may be obtained
from the Defense Documentation Center, Cameron
Station, Alexandria, Virginia 22314.

| | |
|---------------------------------|--|
| ACCESSION FOR | White Section <input type="checkbox"/> |
| NTIS | Dark Section <input checked="" type="checkbox"/> |
| DIC | <input type="checkbox"/> |
| UNCLASSIFIED | |
| AMPLIFICATION | |
| BY | |
| DISTRIBUTION/AVAILABILITY CODES | |
| Dist | Avail. and/or Control |
| B | |

The findings in this report are not to be construed as
an official Department of the Army position, unless
so designated by other authorized documents.

UNCLASSIFIED

SECURITY CLASSIFICATION OF THIS PAGE (When Data Entered)

| REPORT DOCUMENTATION PAGE | | READ INSTRUCTIONS BEFORE COMPLETING FORM |
|---|-------------------------|---|
| 1. REPORT NUMBER BRL Memorandum Report No. 2509 | 2. GOVT ACCESSION NO. ✓ | 3. RECIPIENT'S CATALOG NUMBER |
| 4. TITLE (and Subtitle) Calculations of Fragment Velocities from Naturally Fragmenting Munitions | | 5. TYPE OF REPORT & PERIOD COVERED BRL Memorandum Report |
| | | 6. PERFORMING ORG. REPORT NUMBER |
| 7. AUTHOR(s) R. R. Harpp W. W. Predebon | | 8. CONTRACT OR GRANT NUMBER(s) N/A |
| 9. PERFORMING ORGANIZATION NAME AND ADDRESS US Army Ballistic Research Laboratories, Aberdeen Proving Ground, MD 21005 ✓ | | 10. PROGRAM ELEMENT, PROJECT, TASK AREA & WORK UNIT NUMBERS Proj. Element 61102A Proj. No: 1T161102A33H |
| 11. CONTROLLING OFFICE NAME AND ADDRESS US Army Materiel Command 5001 Eisenhower Avenue Alexandria, VA 22333 | | 12. REPORT DATE Jul 75 (13) 31 p. |
| 14. MONITORING AGENCY NAME & ADDRESS (if different from Controlling Office) (16) DA-1-T-1621 Q2-A-EE-11 | | 13. NUMBER OF PAGES 39 |
| | | 15. SECURITY CLASS. (of this report) Unclassified |
| | | 15a. DECLASSIFICATION/DOWNGRADING SCHEDULE N/A |
| 16. DISTRIBUTION STATEMENT (of this Report) Distribution limited to US Government agencies only; Test and Evaluation; July 1975. Other requests for this document must be referred to Director, USA Ballistic Research Laboratories, ATTN: AMYBR-SS, Aberdeen Proving Ground, Maryland 21005. | | |
| 17. DISTRIBUTION STATEMENT (of the abstract entered in Block 20, if different from Report) | | |
| 18. SUPPLEMENTARY NOTES | | |
| 19. KEY WORDS (Continue on reverse side if necessary and identify by block number) Fragmentation Finite-Difference Codes Fragment Velocity Predictions | | |
| 20. ABSTRACT (Continue on reverse side if necessary and identify by block number) Calculational techniques for predicting warhead performance based upon the fragment velocity distribution are presented and compared with experimental data. A simple technique is shown to be inadequate for many practical configurations. For accurate distributions, a two-dimensional, time-dependent, finite-difference code is shown to be adequate. As an integral part of this code, a model for the effects of casing fragmentation and explosive gas leakage has been included. | | |

DD FORM 1 JAN 73 1473

EDITION OF 1 NOV 65 IS OBSOLETE

UNCLASSIFIED

SECURITY CLASSIFICATION OF THIS PAGE (When Data Entered)

050 750

TABLE OF CONTENTS

| | <u>PAGE</u> |
|---|-------------|
| LIST OF FIGURES | 5 |
| I. INTRODUCTION | 7 |
| II. APPLICABILITY OF THE GURNEY AND TAYLOR FORMULAE | 7 |
| III. EFFECT OF GAS LEAKAGE AFTER CASING BREAKUP. | 8 |
| IV. USE OF TIME-DEPENDENT, TWO-DIMENSIONAL, FINITE- DIFFERENCE CODES | 9 |
| 1. Equation of State of the Explosive | 9 |
| 2. Problems Associated With Determination of a Final Fragment Velocity | 9 |
| 3. Final Fragment Velocities Using a Gas Leakage Model | 10 |
| 4. Comparisons of Code Calculations with Experimental Results | 11 |
| V. SUMMARY AND RECOMMENDATIONS. | 12 |
| VI. APPENDIX A - FIGURES | 15 |
| DISTRIBUTION | 37 |

LIST OF FIGURES

| <u>Figure</u> | | <u>Page</u> |
|---------------|--|-------------|
| 1 | Gurney Velocity Formula (Cylinder) and Taylor's Projection Angle Formula. | 16 |
| 2 | Comparison of Gurney and Taylor Formulae Predictions With Experimental Data, Case 1. | 17 |
| 3 | Comparison of Gurney and Taylor Formulae Predictions With Experimental Data, Case 2. | 18 |
| 4 | LLL Standard Cylinder Test. | 19 |
| 5 | Comparison of the Rate of Expansion versus Expansion Ratio for Various Explosive Fills (Ref. 3). | 20 |
| 6 | Comparison of Rate of Expansion versus Displacement for Various Casing Materials (Ref. 3) | 21 |
| 7 | Cylinder Expansion and Measured Values of Expansion Ratios for Various Casing Materials at which Gas Leakage Occurs (Ref. 4) | 22 |
| 8 | HEMP Calculations Using the JWL Equation of State of the Explosive as Indicated Above Compared with the Data from the LLL Standard Cylinder Test. | 23 |
| 9 | Finite-Difference Mesh Used in the HEMP Calculations of the LLL Standard Cylinder Test | 24 |
| 10 | Computer Simulation of an Open Ended Steel Cylinder with an Octol Explosive Fill. | 25 |
| 11 | Comparison of Fragment Speed Versus Time at Two Positions on the Casing Wall Using the Fluid, Elastic-Plastic and Elastic-Plastic with Gas Leakage Models. | 26 |
| 12 | Notation for Gas Leakage Model. | 27 |
| 13 | Comparison Between HEMP Calculations and Experimental Data of Fragment Speed and Projection Angle for Cylinders of L/D = 2, Octol, C/M = .8 | 28 |
| 14 | Comparison Between HEMP Calculations and Experimental Data of Fragment Speed and Projection Angle for Cylinders of L/D = 2, Composition B, C/M = .8 | 29 |

LIST OF FIGURES

| <u>Figure</u> | | <u>Page</u> |
|---------------|---|-------------|
| 15 | Comparison Between HEMP Calculations and Experimental Data of Fragment Speed and Projection Angle for Cylinders of L/D = 2, TNT, C/M = .8 | 30 |
| 16 | Comparison Between HEMP Calculations and Experimental Data of Fragment Speed and Projection Angle for Cylinders of L/D = 2, Octol, C/M = .4 | 31 |
| 17 | Comparison Between HEMP Calculations and Experimental Data of Fragment Speed and Projection Angle for Cylinders of L/D = 2, Composition B, C/M = .4 | 32 |
| 18 | Comparison Between HEMP Calculations and Experimental Data of Fragment Speed and Projection Angle for Cylinders of L/D = 2, TNT, C/M = .4 | 33 |
| 19 | Comparison Between HEMP Calculations and Experimental Data Obtained From Arena Tests - Fragment Speed versus Angular Position | 34 |
| 20 | Comparison Between HEMP Calculations and Experimental Data Obtained From Arena Tests - Fragment Mass versus Angular Position | 35 |

I. INTRODUCTION

Accurate modeling as well as predicting the performance of naturally fragmenting munitions is particularly important to the Army munitions community. For parametric studies, calculational techniques which are both quick and easy to use are of practical interest. One well known technique employs the Gurney¹ and Taylor² formulae. In Section II the advantages and disadvantages of this technique are demonstrated.

In Section III the importance of gas leakage after casing breakup is discussed with the use of the LLL standard cylinder test³ data and experimental observations of a variety of test warhead firings.

In Section IV the use of a time-dependent, two dimensional, finite-difference code, HEMP, to predict fragment velocities is discussed in detail. Problems associated with determining a definite final fragment velocity are mentioned. In an effort to model casing acceleration realistically, a gas leakage model is presented as an integral part of the code calculations. Lastly, the code calculations are compared with a number of experimental test results.

II. APPLICABILITY OF THE GURNEY AND TAYLOR FORMULAE

Practically speaking, it is desirable to have a method available for estimating fragment velocities from naturally fragmenting munitions which is both quick and easy to use for parametric studies. One such method for estimating fragment velocity is the Gurney¹ formula (Figure 1) which gives the fragment speed as a function of the charge to metal ratio (mass of explosive/mass of casing) and an empirically determined constant. The direction that the fragment assumes can then be determined by the Taylor² formula (Figure 1) using this calculated speed. For an axisymmetric explosive-metal system with variable diameter, the charge to metal ratio (C/M) is computed locally as a function of axial position. Thus, the speed computed from the Gurney formula varies with axial position. In the Taylor formula for the projection angle, both the fragment speed and the rate at which the detonation wave traverses the casing varies with axial position.

1. Gurney, R.W., "The Initial Velocities of Fragments From Bombs, Shells and Grenades", BRL Report 405, September 1943. AD #36218

2. Birkhoff, G., MacDougall, P., Pugh, E.M., and Taylor, G.I., Sir., "Explosives With Lined Cavities", J. Appl. Phys., Vol. 19, p. 563, June 1948.

3. Lee, E.L., Hornig, H.C., and Kury, J.W., "Adiabatic Expansion of High Explosive Detonation Products", UCRL-50422, May 2, 1968.

Numerous comparisons between calculated fragment velocities using the Gurney and Taylor formulae and experimental test results have been made by us and other researchers. For a practical range of charge to metal ratios ($.1 < C/M < 2$), it is our observation that speeds and directions thus calculated agree reasonably well with experimental data for configurations when the flow is essentially radial. Figure 2 illustrates the results of a comparison of the above technique with experimental data for a typical H.E. projectile. The agreement with this test data is quite good. A second example of the agreement between the results of this technique and experimental data is shown in Figure 3. Here a steel cylinder with length to diameter ratio of two filled with Composition B explosive and initiated on axis at one end is shown. Here the agreement is not good. This figure illustrates the degree to which end effects may influence the fragment speed distribution and projection angle distribution. One can see that a method which can predict both the fragment speed and direction distributions correctly is desirable. That is, a method which will model general time-dependent, two-dimensional phenomena, such as end effects, with some degree of confidence would be a useful tool. The method proposed and utilized in this report is a modified version of the time-dependent, two-dimensional, finite-difference computer code, HEMP.

III. EFFECT OF GAS LEAKAGE AFTER CASING BREAKUP

The standard cylinder test³ developed by the Lawrence Livermore Laboratory, Livermore, California, provides much data concerning the expansion of explosive-filled cylinders. Figure 4 schematically illustrates the test procedure. The radial expansion of the copper cylinder is measured with a streak camera at a point two-thirds the length of the cylinder from the initiated end. The rate of expansion of the cylinder is plotted in Figure 5 as a function of radial displacement and expansion ratio for three different explosive fills, Octol, Composition B and TNT. The percentages indicated on the curves signify the percent of the final expansion rate. During these measurements, neither significant leakage of explosive products nor influence of end effects occurs. The general shape of the curves are of interest since they indicate that most of the acceleration has occurred by an expansion ratio of $R/R_0 = 2$. Even at $R/R_0 = 1.75$ at least 92% of the final velocity has already been obtained. These curves are for copper casings; however, Figure 6 (taken from Reference 3) indicates that the shape of the curve is the same for stainless steel and mild steel; the latter is important for naturally fragmenting, steel casing munitions.

Gas leakage has been experimentally observed at an expansion ratio of about $R/R_0 = 1.75$ for many steels.^{4,5} Figure 7 lists such observed values of R/R_0 for steel, copper, and aluminum casings. Even though about 92% or more of the final casing velocity is acquired before casing breakup for natural fragmentation; we will show in Section IV that it is desirable to include the effects of gas leakage in time dependent calculations to obtain accurate predictions of fragment velocities particularly in regions influenced by end rarefaction waves.

IV. USE OF TIME-DEPENDENT, TWO-DIMENSIONAL, FINITE-DIFFERENCE CODES

1. Equation of State of the Explosive

The Jones, Wilkins, Lee (JWL) equation of state recommended in Reference 3 and given in Figure 8 is used in these calculations. The finite-difference code used in the present work is the HEMP code⁶. However, equally good results could be obtained with other valid finite-difference codes⁷.

The JWL equations of state are developed such that the radial expansion rate obtained from the LLL standard cylinder test can be duplicated with a HEMP calculation. Figure 8 indicates the accuracy with which the finite-difference calculations reproduce the data. Figure 9 shows the finite-difference mesh which was used to compare with the LLL standard cylinder test data. In general, good agreement between HEMP code calculations, experiments, and exact analytical solutions has been demonstrated.⁸

2. Problems Associated With Determination of a Final Fragment Velocity

Figure 10 shows the finite-difference mesh at various times for a HEMP calculation of an open ended steel cylinder with an Octol

4. Taylor, G.I., "The Fragmentation of Tubular Bombs", Scientific Papers of G.I. Taylor, Vol. III, Cambridge University Press, London, 1963.

5. Hoggatt, C. and Recht, R., "Fracture Behavior of Tubular Bombs", J. Appl. Phys., Vol. 39, pp. 1856 - 1862, February 1968.

6. Wilkins, M.L., "Calculation of Elastic-Plastic Flow", Methods of Computational Physics, Vol. 3, edited by Alder, B., Fernbach, S. and Rotenburg, M., Academic Press, New York, 1964.

7. Sedgwick, R.T., A.J. Good, and L.J. Hageman, "Theoretical Investigation of High Explosive Fragmentation Munitions", Final Report, Contract DAAD 05-71-C-0092, Systems, Science, and Software Report 3SR-867, Nov. 24, 1971.

8. Karpp, R.R., "Accuracy of HEMP Code Solutions", BRL Memo Report 2268, January 1973. AD #757153

explosive fill. The steel casing can be modeled in several ways. One way is to treat the casing as a fluid (neglect the strength of the steel). This method produces the velocity* - time curves shown in Figure 11 (solid curve). The early portion of the acceleration curve is essentially correct. However, since it is known that a steel cylinder will fragment at an expansion ratio of about 1.75, the latter portion of the acceleration curve will tend to over estimate the final fragment velocity. This effect is a result of the code requiring the casing to be continuous, and, therefore, the internal pressure acts on a continuously increasing area and produces an unrealistically high fragment velocity. Referring to Figure 11, this effect is more pronounced at position 1, where end effects are important, than at position 2. Therefore, the calculational results with the fluid model will tend to over-estimate the final fragment velocity. Since the velocity continually increases, one must use an artificial method to determine the correct final fragment velocity distribution. A second method of modeling the casing includes the material strength of the casing. This can be done by modeling the metal casing as an elastic-plastic material. A curve showing the velocity-time plot when the casing is treated as an elastic-perfectly plastic material is given in Figure 11 (dot-dash curve). This model does produce a more definite value for the final fragment velocity. However, this maximum value for fragment velocity still occurs at an expansion ratio considerably beyond the known expansion ratio at fragmentation. Besides the fluid model objection which also applies to this model, it does not seem realistic to include strength in the calculations past the point where the casing fragments. A calculational procedure which does not rely on an artificial method to determine the final fragment velocity but includes the appropriate physics of fragmentation and subsequent gas leakage is discussed in the next section.

3. Final Fragment Velocities Using a Gas Leakage Model

Several features of the warhead expansion and fracture process are inadequately modeled by axisymmetric finite-difference computer codes when casing breakup occurs. First, the increase in circumference ceases when casing fragmentation occurs. The standard form of these codes causes the casing to remain continuous. This treatment tends to yield a higher radial acceleration and thus higher final fragment velocity since the pressure acts on an area which is larger than the true area. However, this effect can be corrected by calculating the true force acting on an element of the casing. After casing fragmentation ($R > R_b$) the true force is calculated by reducing the pressure acting on the interface of the casing by the factor R_b/R (Refer to Figure 12).

** Velocity as used in conjunction with any of the Figures given is the magnitude of the velocity. When the direction of the velocity is discussed or plotted it is referred to as projection angle.*

Secondly, after casing fragmentation, i.e. $R > R_p$, a void area A_L opens up and gas leakage occurs. This effect is modeled by calculating the rate of efflux from an ideal nozzle passing its maximum rate of flow. For example, for an ideal gas the mass rate of flow is given by

$$\dot{m} = A_L \sqrt{\gamma P \rho} \left(\frac{2}{\gamma + 1} \right)^{\frac{\gamma + 1}{2(\gamma - 1)}}$$

Where P is pressure, ρ is density and γ is the ratio of specific heats. This rate of efflux is calculated in the model for every cycle and the mass leaked for a single cycle is $\Delta m = \dot{m} \Delta t$. The amount of mass (Δm) is then extracted from the zone in contact with the casing interface. In this manner, the model accounts for gas leakage around the fragments after casing breakup. Thirdly, to simulate a loss in circumferential stress upon casing breakup, the yield strength of the casing material is set equal to zero when $R > R_p$.

A comparison of the three casing models discussed, i.e. fluid, elastic-plastic and elastic-plastic with gas leakage, is shown in Figure 11. Here the velocity-time curves are given for two positions along the casing, namely, close to the initiation end and at the maximum velocity position. Figure 11 clearly shows that a more definite and lower final fragment velocity is obtained by modeling the casing material as an elastic-plastic material and accounting for gas leakage.

4. Comparisons of Code Calculations with Experimental Results

In this section we present comparisons of the code calculations, utilizing the gas leakage model, with a number of experimental test results to demonstrate the reliability of this calculational technique. In Figures 13 through 18 the HEMP code predictions of fragment speed and projection angle are compared with experimental test results. The HEMP code calculations of fragment speed and projection angle are plotted as continuous curves in all the figures. The experimental data are plotted according to round numbers in each case. For information concerning the experimental set up, data collection and test firings, the reader is referred to Reference 9 for details. For each of the six cases represented in Figures 13 through 18 the length to diameter ratio was two, and they were end initiated as shown in Figure 13. The explosive fills were Octol, Composition B, and TNT, and the casing was 1020 steel or HF-1 steel. The charge to metal ratio

9. Karpp, R.R., Kronman, S., Dietrich, A.M. and Vitali, R., "Influence of Explosive Parameters on Fragmentation", BRL Memorandum Report 2330, October 1973. AD #917248L

was 0.8 (thin wall) for the cases shown in Figures 13-15 and 0.4 (thick wall) in Figures 16 - 18. No discussion will be given here concerning the experimental data as it is covered in detail in Reference 9. However, we do wish to emphasize the good agreement between experimental results and the calculations for a variety of explosive fills and C/M ratios.

Lastly, in Figures 19 and 20 HEMP calculations are again compared with test data. However, in this case the test data are from "arena tests" of an H.E. projectile.¹⁰ In Figure 19 the fragment velocity is plotted against angular position in the arena test set up. In Figure 20 the percent recovered mass in each angular recovery position is plotted. Again, very good agreement is demonstrated.

V. SUMMARY AND RECOMMENDATIONS

In the first part of the report it was shown that fragment velocity predictions based on the Gurney and Taylor formulae may be adequate for cases when the flow is one-dimensional (radial), but inadequate when the flow becomes two-dimensional. It was then shown from the LLL standard cylinder tests that in the natural fragmentation case most of the casing velocity is obtained prior to fragmentation. Next the use of a time-dependent, two-dimensional, finite-difference code, HEMP, to model naturally fragmenting munitions was discussed. Arguments were given to show that the fluid model (without strength) for the casing material will tend to over-estimate the final fragment velocity. The casing material modeled as an elastic-plastic material tends to produce a more definite final fragment velocity, but at unrealistically high cylinder expansions. In an effort to remove some of these objections and at the same time model the casing motion more realistically, a gas leakage model was proposed in conjunction with the code calculations. The gas leakage model was designed to simulate explosive gas leakage around fragments after casing breakup. Comparisons are given between the code calculations with the gas leakage model and experimental data, and very good agreement was demonstrated. However, we wish to emphasize that the gas leakage model presented is still in its early development. Further modifications and improvements are planned. Based on the agreement shown between the code calculations and the experimental test cases given, it is our judgement that this calculational tool can be used confidently in a variety of naturally fragmenting munitions when experimental data is not available.

Our future efforts will include the development of a more general criterion to initiate the gas leakage based on the state of stress

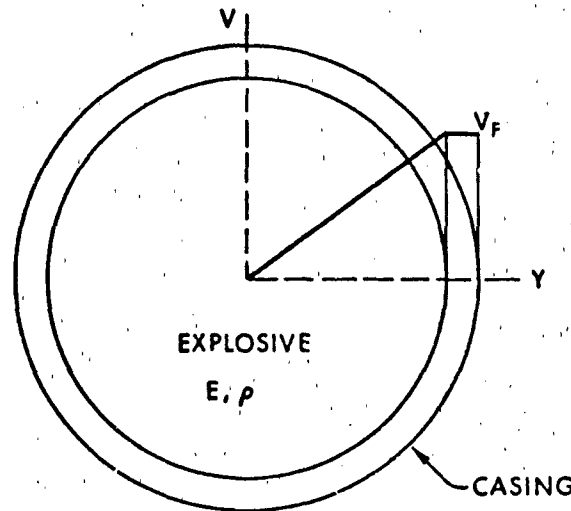
10. U.S. Army TECOM Development and Proof Services, Firing Record No. B11982, Aberdeen Proving Ground, Maryland, August 1953 to June 1954.

in the casing material, rather than on the expansion ratio. Lastly, some effort has already been expended and much more is planned to investigate the use of the HEMP calculations to model fragment velocities from preformed¹¹ and controlled fragmentation warheads using the proposed gas leakage model.

11. Karpp, R.R., and Predebon, W.W., "Calculation of Fragment Velocities from Fragmentation Munitions" *First International Symposium on Ballistics, Orlando, Fla., 13-15 November 1974, Section IV, pp. 145-176, American Defense Preparedness Association, Washington, D.C.*

VI. APPENDIX A: FIGURES

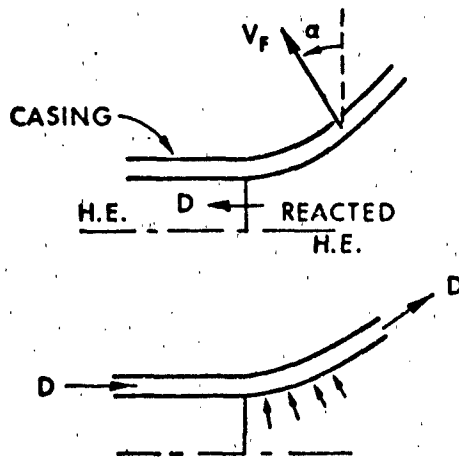
GURNEY'S VELOCITY FORMULA



$$V_F = \sqrt{2E} \left(\frac{C/M}{1 + \frac{1}{2} C/M} \right)^{1/2}$$

(A)

TAYLOR'S PROJECTION ANGLE FORMULA



$$\sin \alpha = \frac{V_F}{2D}$$

(B)

Figure 1. Gurney Velocity Formula (Cylinder) and Taylor's Projection Angle Formula

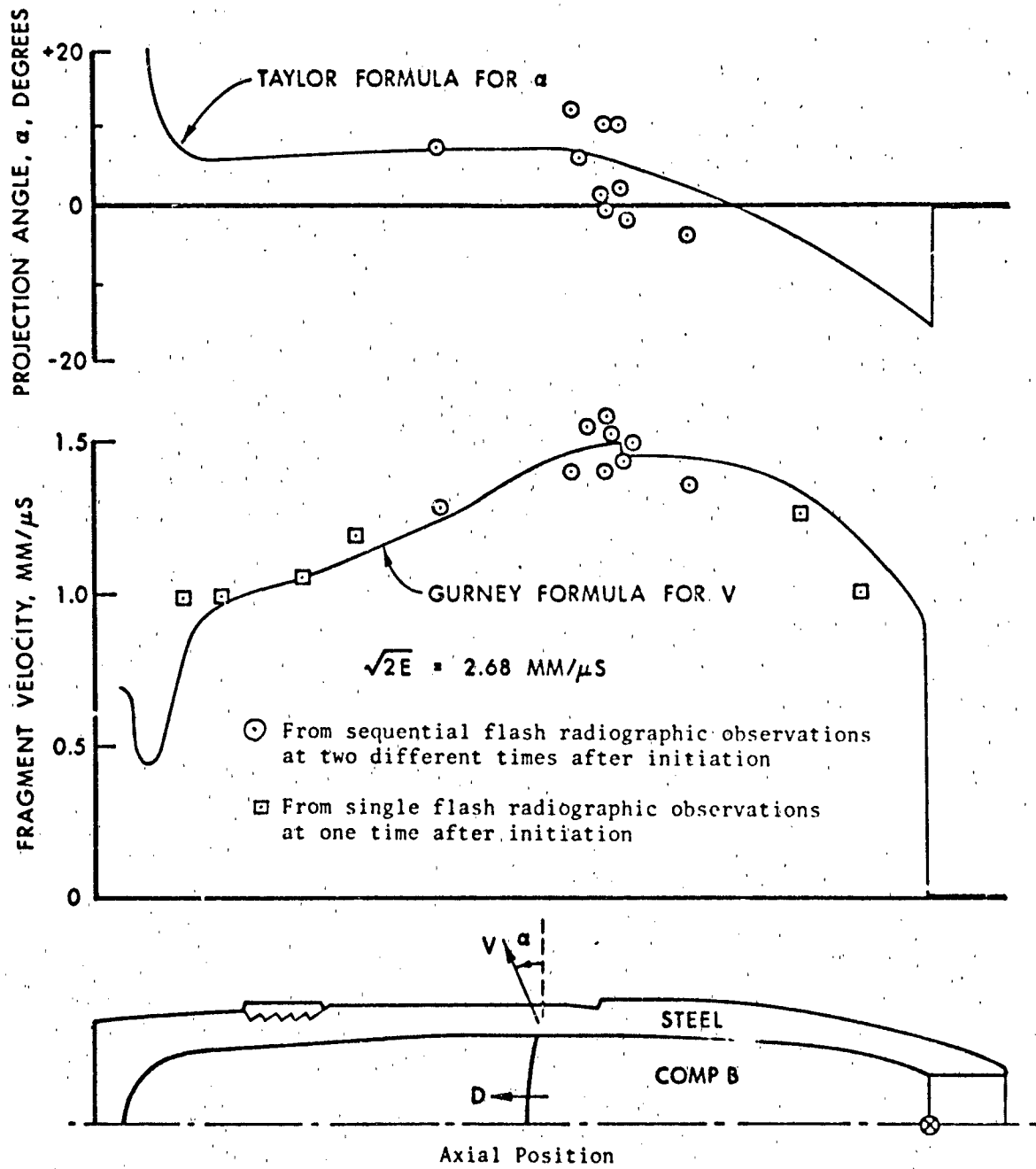


Figure 2. Comparison of Gurney and Taylor Formulae Predictions With Experimental Data, Case 1

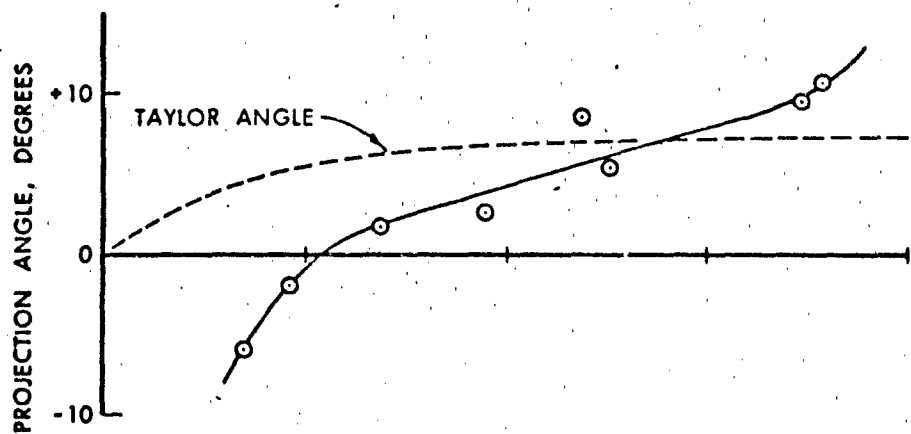
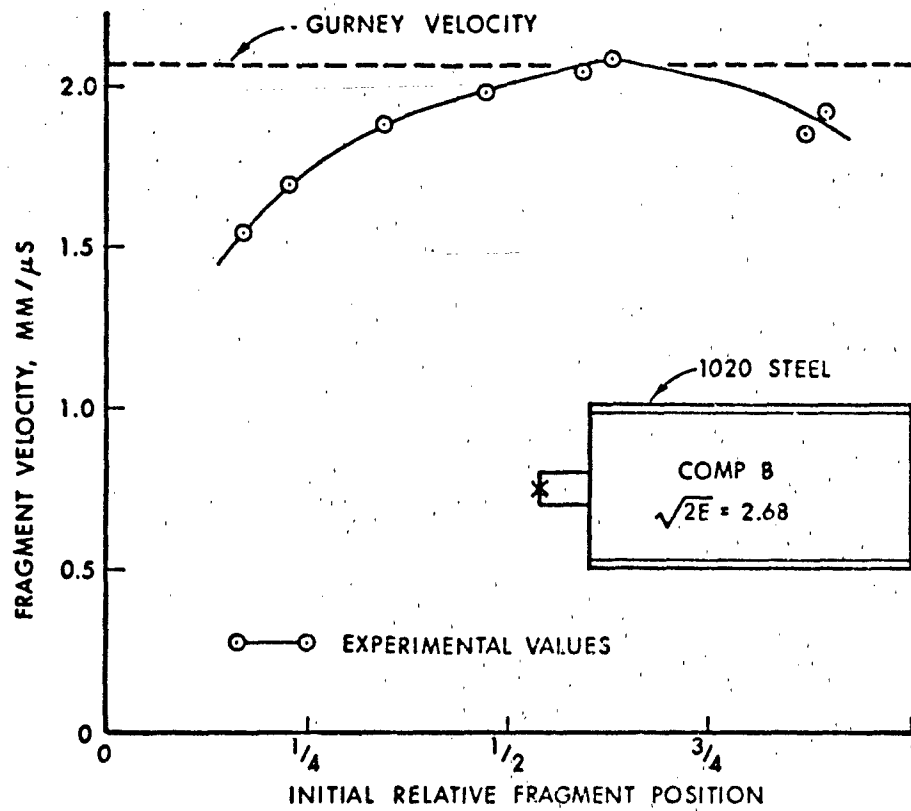


Figure 3. Comparison of Gurney and Taylor Formulae Predictions With Experimental Data, Case 2

LLL STANDARD CYLINDER TEST

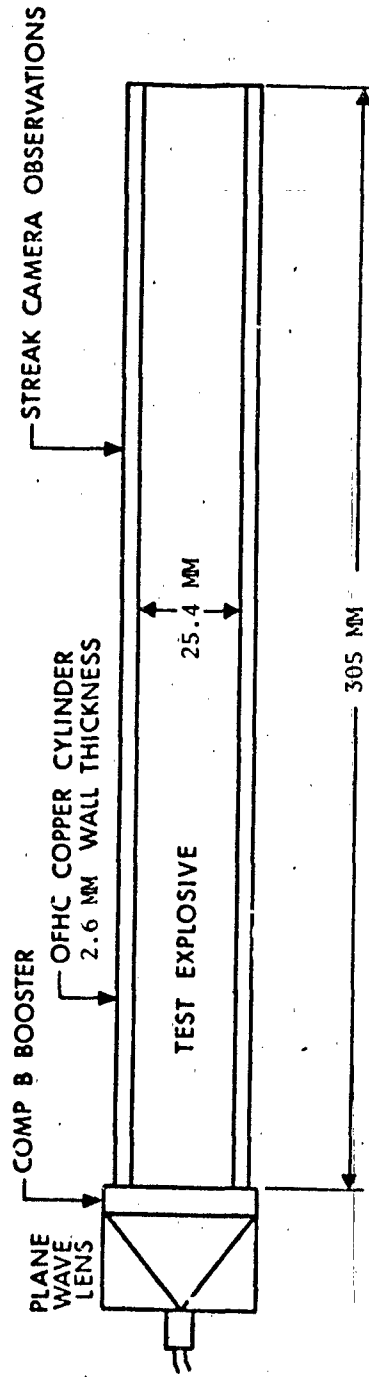


Figure 4. LLL Standard Cylinder Test

STANDARD CYLINDER TEST DATA FROM LLL

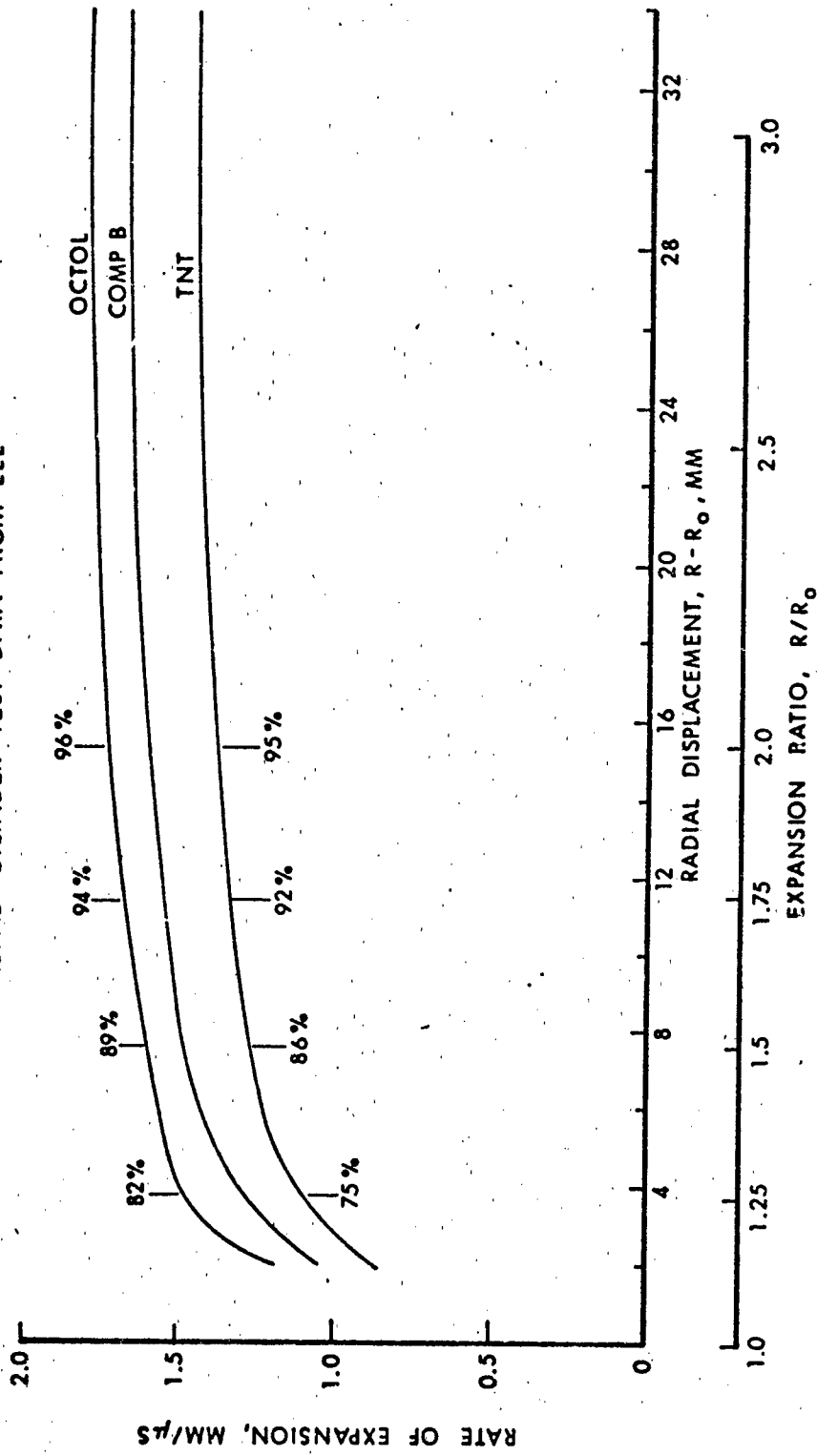


Figure 5. Comparison of the Rate of Expansion Versus Expansion Ratio for Various Explosive Fills (Ref. 3)

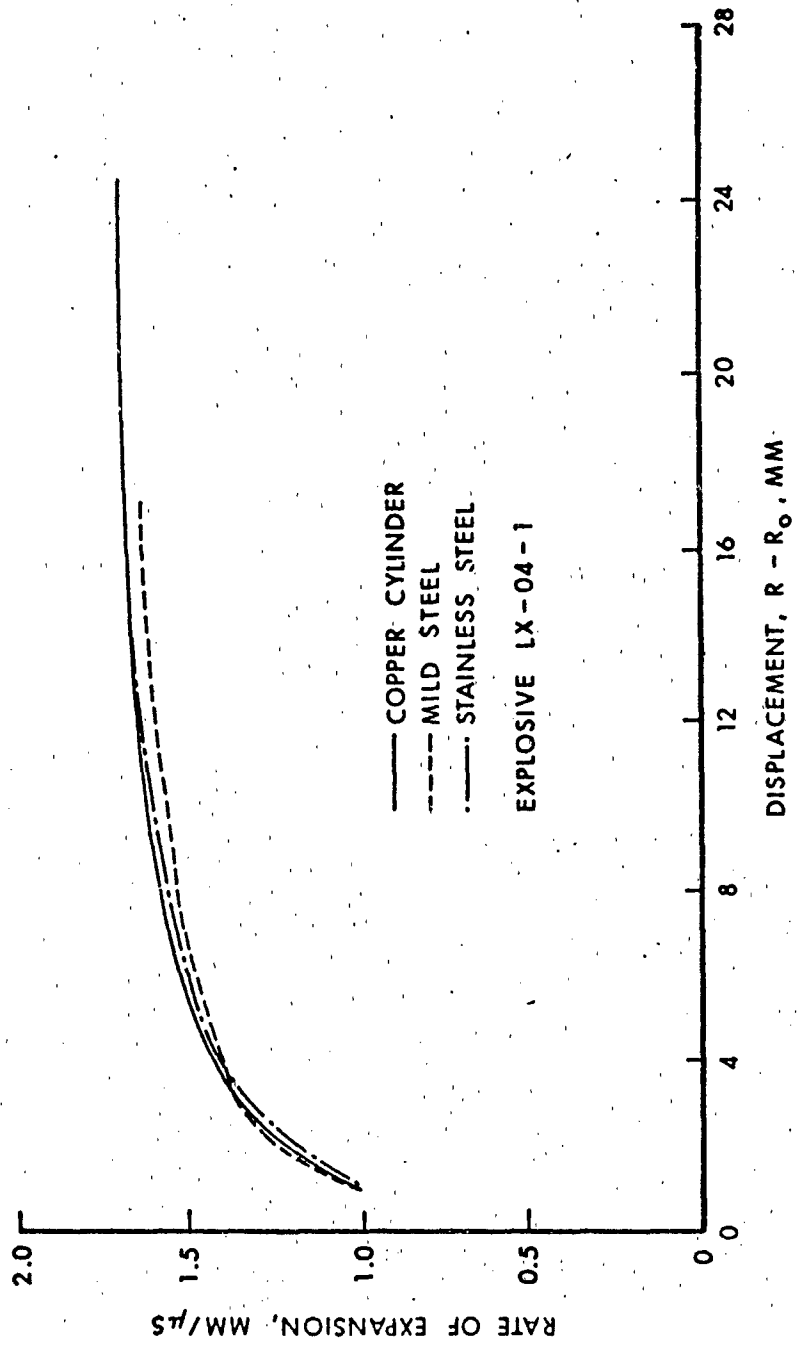
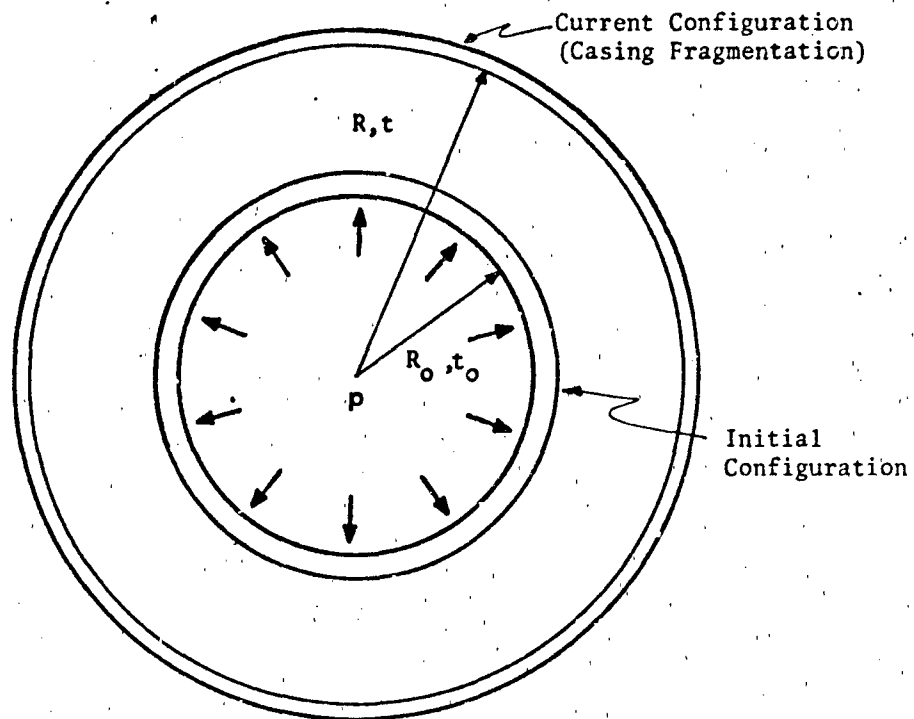


Figure 6. Comparison of Rate of Expansion Versus Displacement for Various Casing Materials (Ref. 3)



| | <u>OBSERVED GAS LEAKAGE AT R/R_0</u> |
|------------------------|---|
| STEEL / VARIOUS H.E.'s | 1.6 TO 2.1 |
| COPPER | 2.4 |
| ALUMINUM | 3.2 |

Figure 7. Cylinder Expansion and Measured Values of Expansion Ratios for Various Casing Materials at which Gas Leakage Occurs (Ref. 4)

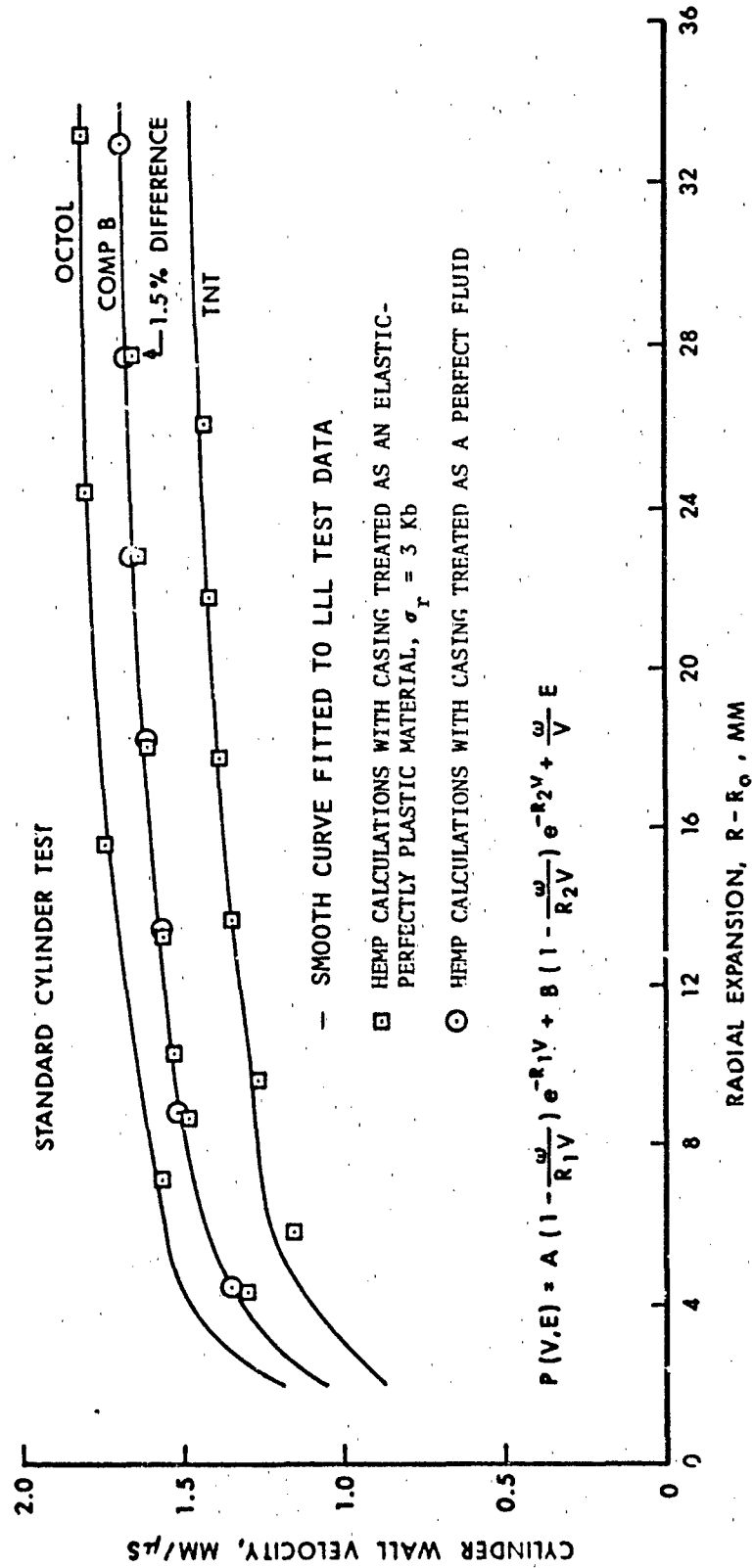
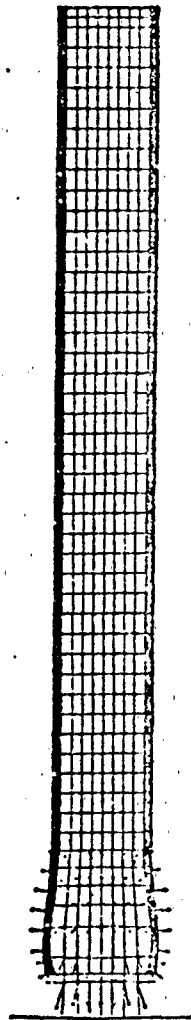
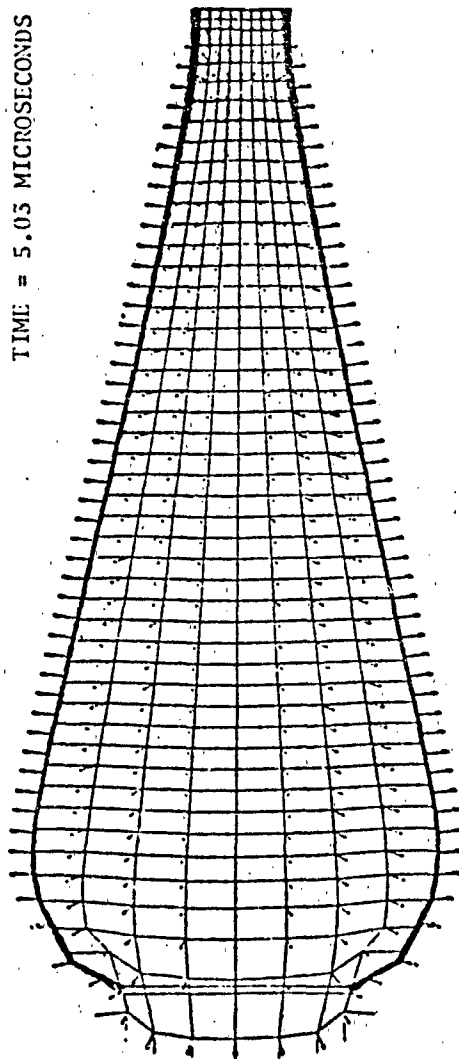


Figure 8. HEMP Calculations Using the JWL Equation of State of the Explosive as Indicated Above Compared with the Data from the LLL Standard Cylinder Test

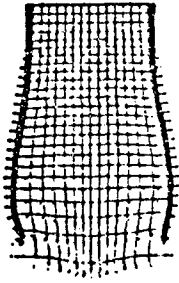


TIME = 5.05 MICROSECONDS

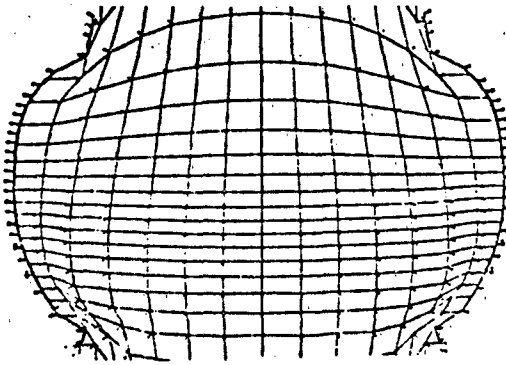


TIME = 35.0 MICROSECONDS

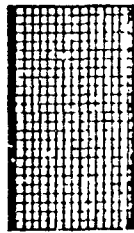
Figure 9. Finite-Difference Mesh Used in the HEMP Calculations of the LLL Standard Cylinder Test



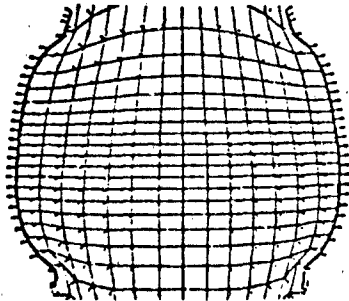
25 MICROSECONDS



125 MICROSECONDS



TIME = 0 MICROSECONDS



TIME = 75 MICROSECONDS

Figure 10. COMPUTER SIMULATION OF AN OPEN ENDED STEEL CYLINDER WITH AN OCTOL EXPLOSIVE TEST

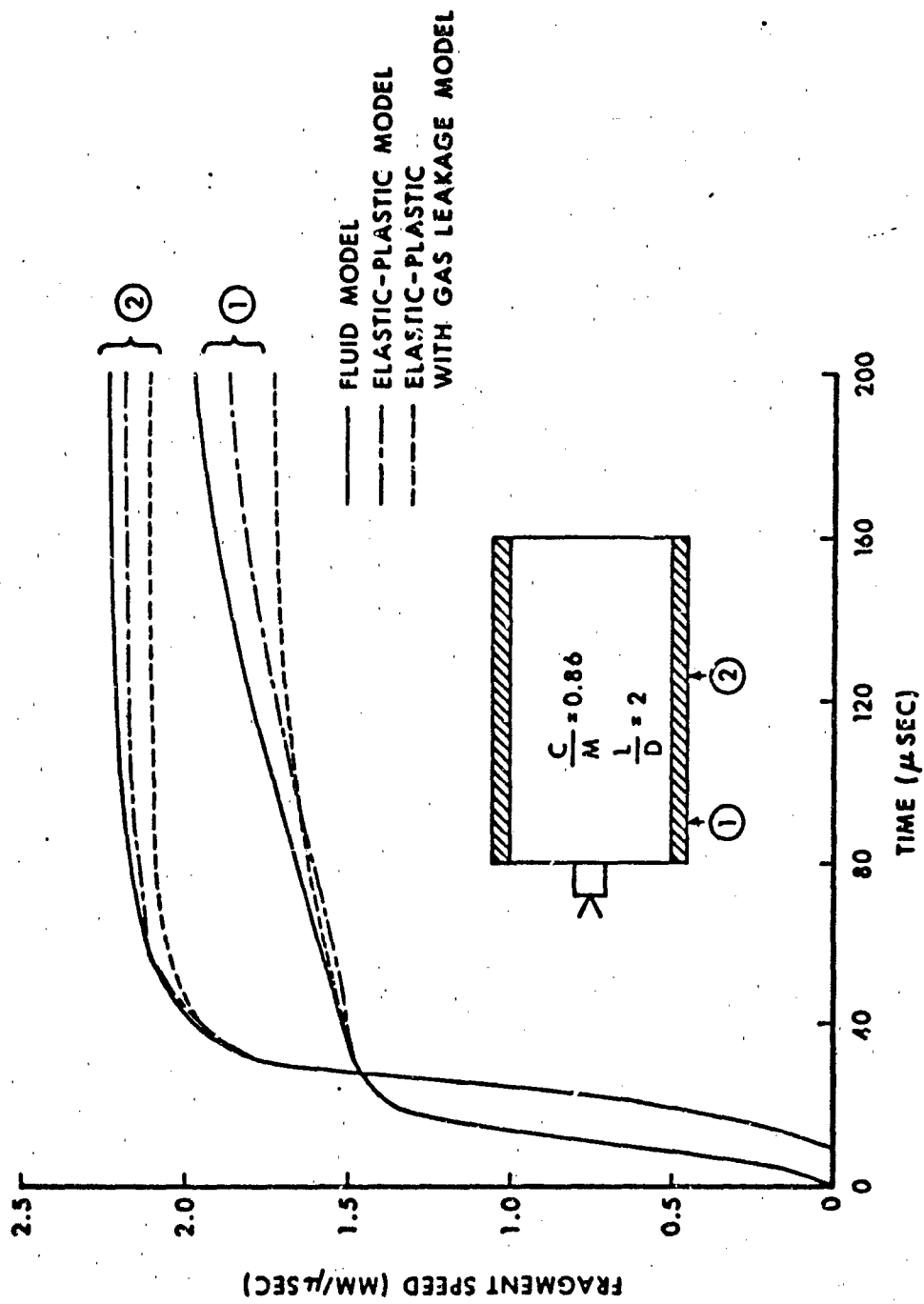
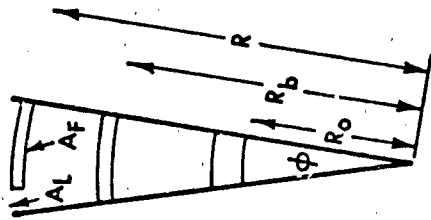


Figure 11. Comparison of Fragment Speed Versus Time at Two Positions on the Casing Wall Using the Fluid, Elastic-Plastic and Elastic-Plastic with Gas Leakage Models



- R_0 - INITIAL CASING RADIUS
- R_b - RADIUS AT FRAGMENTATION
- R - CURRENT RADIUS
- $A_F = R_b \phi$ - FRAGMENT AREA/UNIT LENGTH
- $A_L = (R - R_b) \phi$ - LEAKAGE AREA/UNIT LENGTH

FORCE ON FRAGMENT/UNIT LENGTH =

$$PA_F = P \left(\frac{A_F}{A_L + A_F} \right) (A_L + A_F)$$

$$= \frac{R_b}{R} P (A_L + A_F)$$

= (MODIFIED PRESSURE) (AREA IN CODE)

Figure 12. Notation for Gas Leakage Model

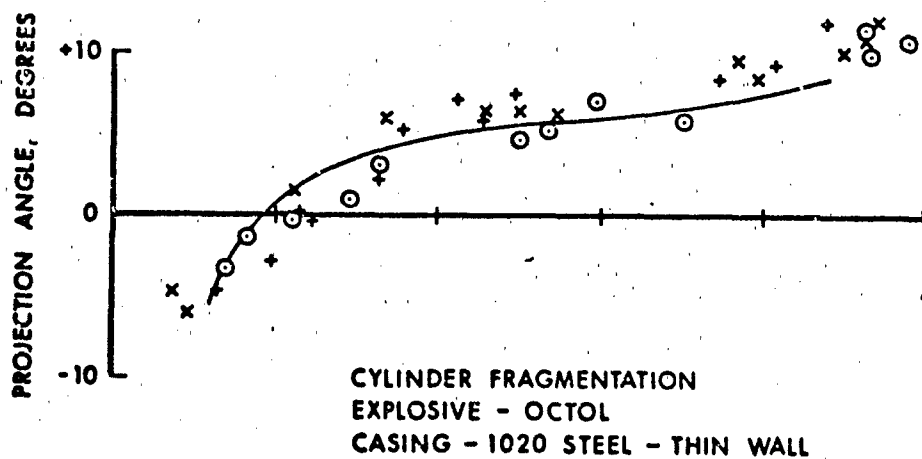
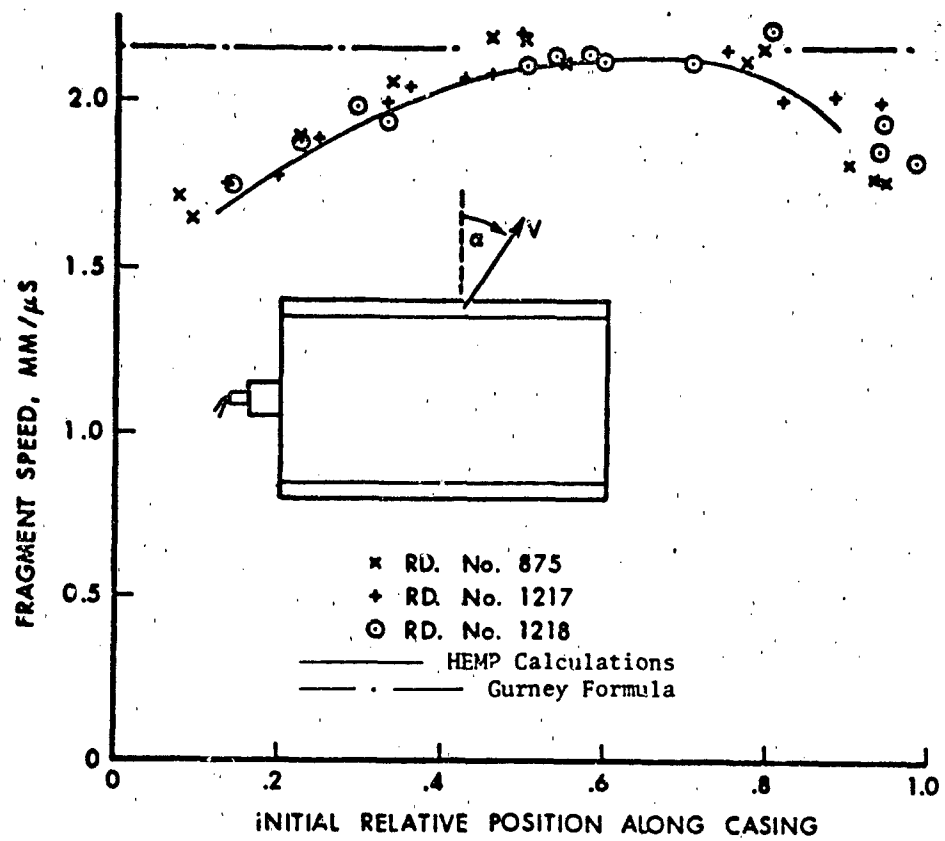


Figure 13. Comparison Between HEMP Calculations and Experimental Data of Fragment Speed and Projection Angle for Cylinders of $L/D = 2$, Octol, $C/M = .8$

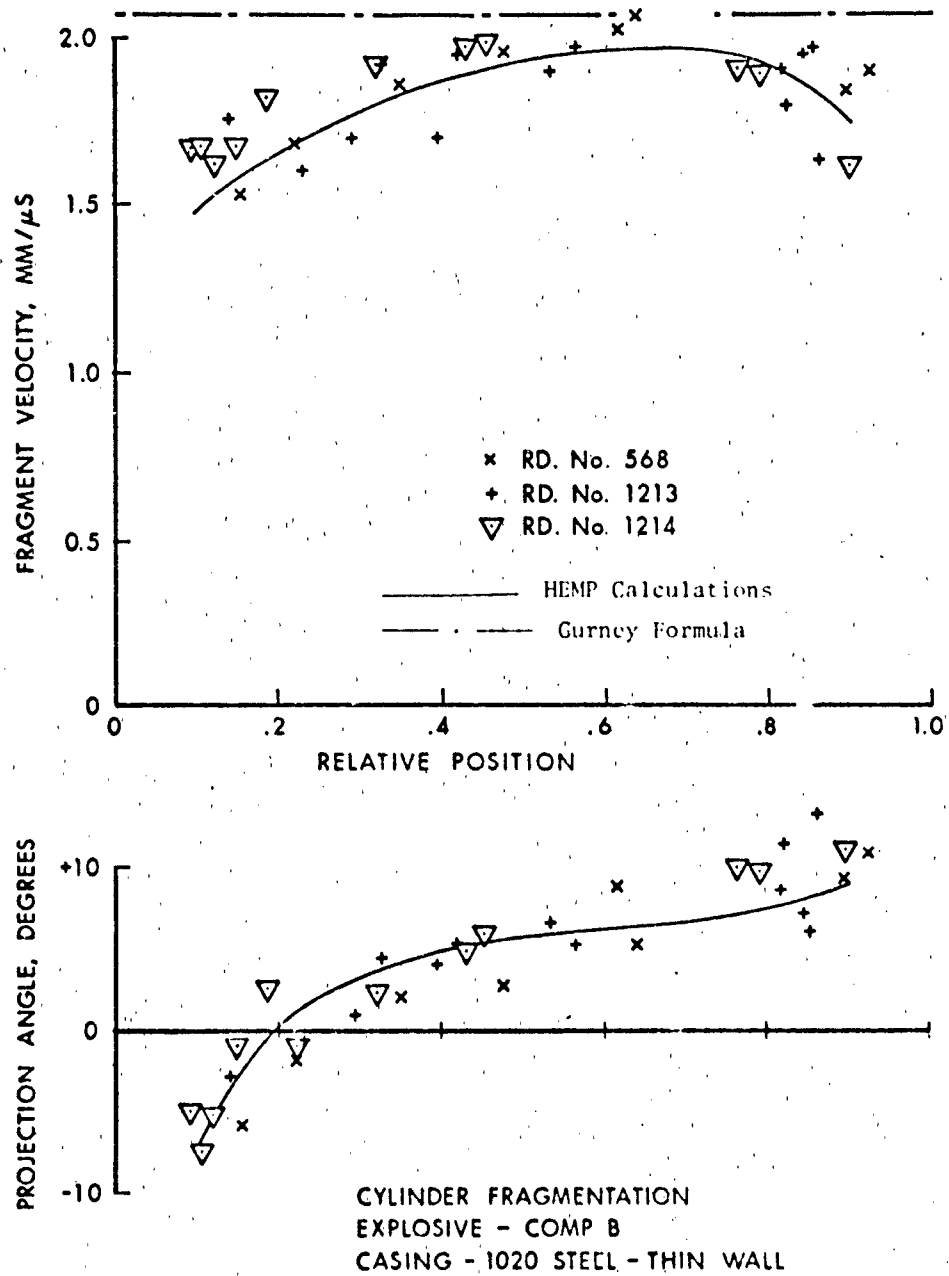


Figure 14. Comparison Between HEMP Calculations and Experimental Data of Fragment Speed and Projection Angle for Cylinders of L/D = 2, Composition B, C/M = .8

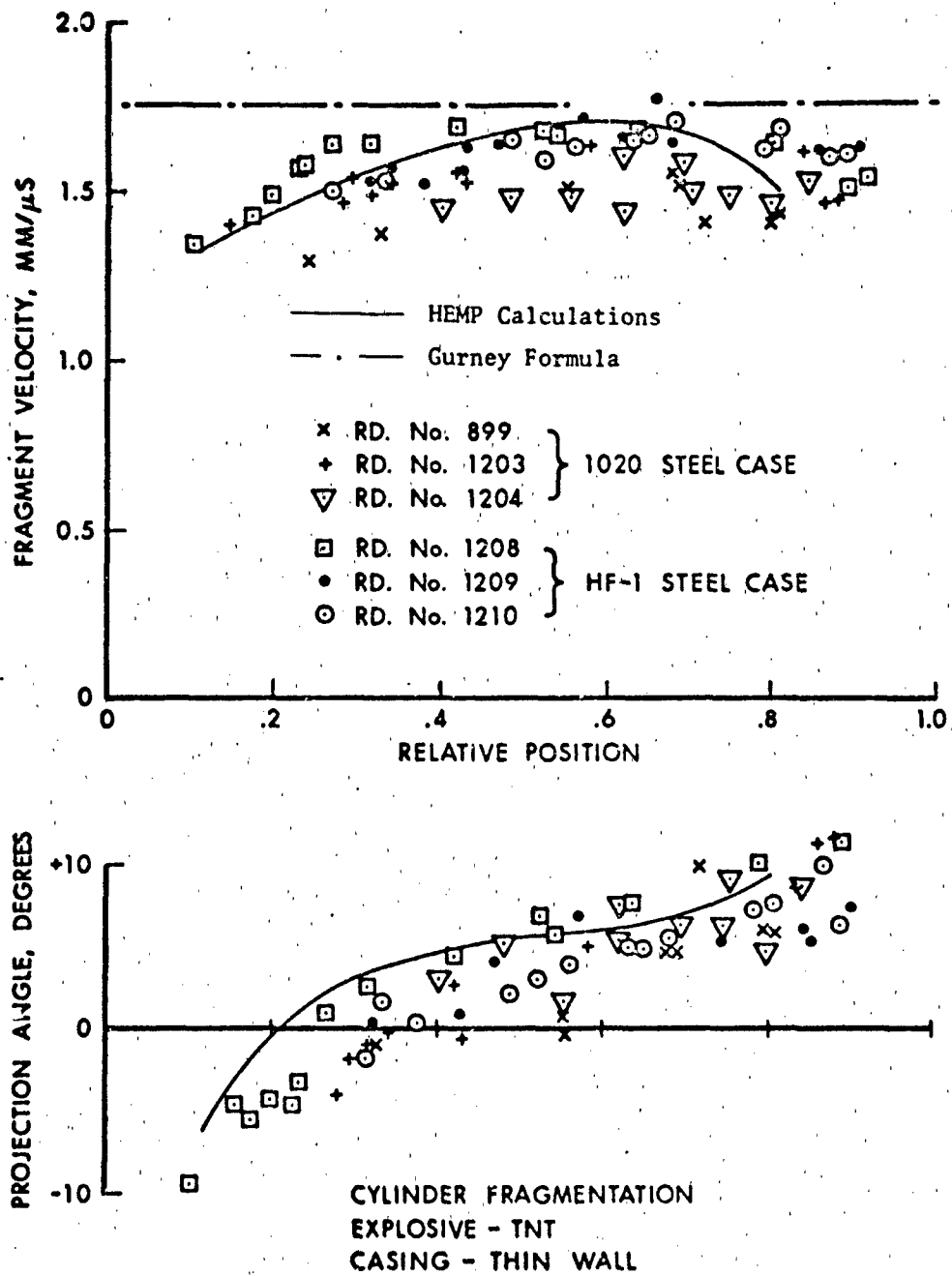


Figure 15. Comparison Between HEMP Calculations and Experimental Data of Fragment Speed and Projection Angle for Cylinders of $L/D = 2$, TNT, $C/M = .8$

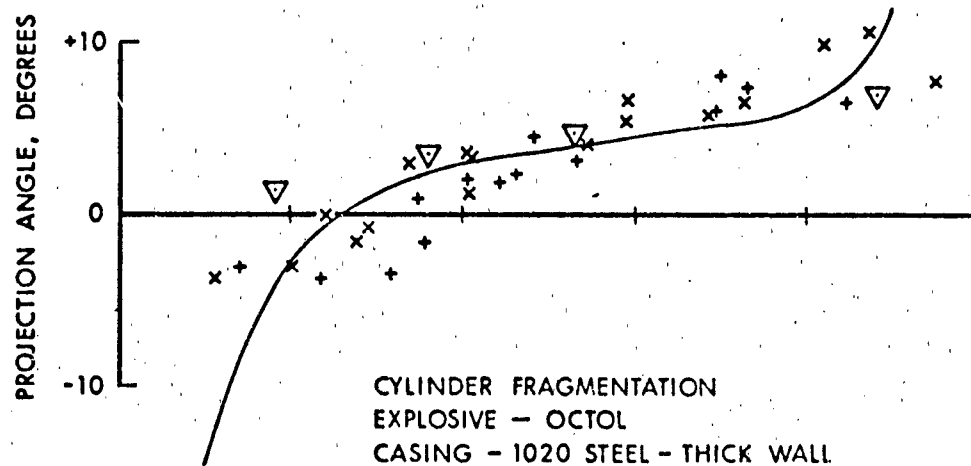
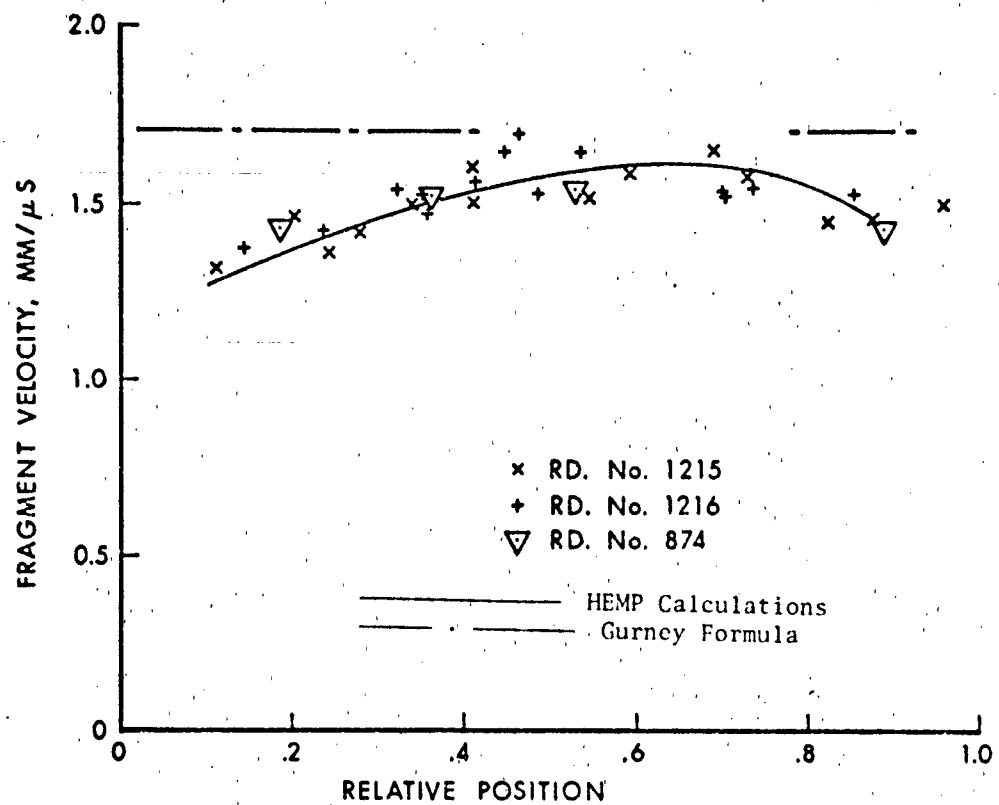


Figure 16. Comparison Between HEMP Calculations and Experimental Data of Fragment Speed and Projection Angle for Cylinders of $L/D = 2$, Octol, $C/M \approx .4$

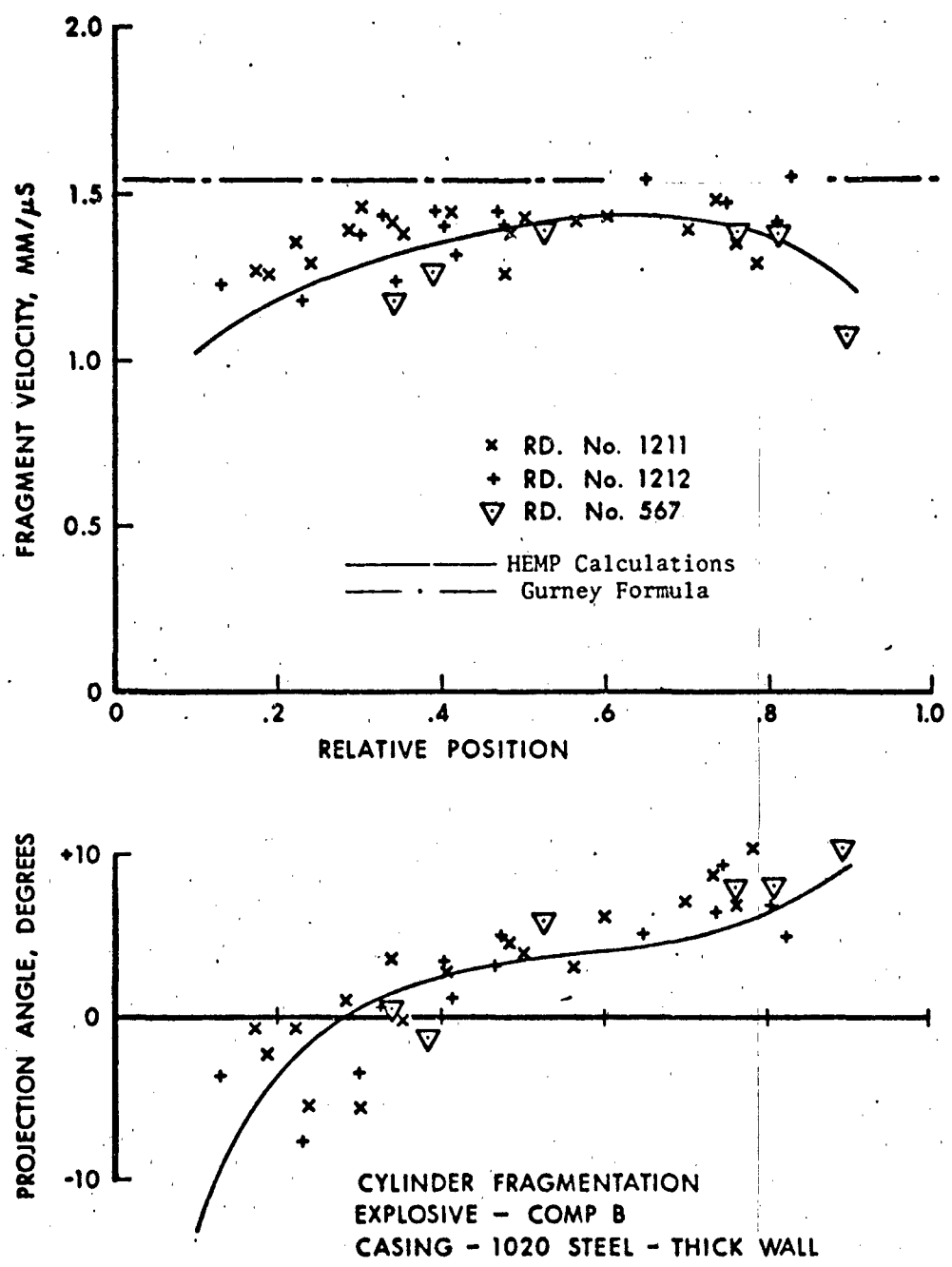


Figure 17. Comparison Between HEMP Calculations and Experimental Data of Fragment Speed and Projection Angle for Cylinders of L/D = 2, Composition B, C/M = .4

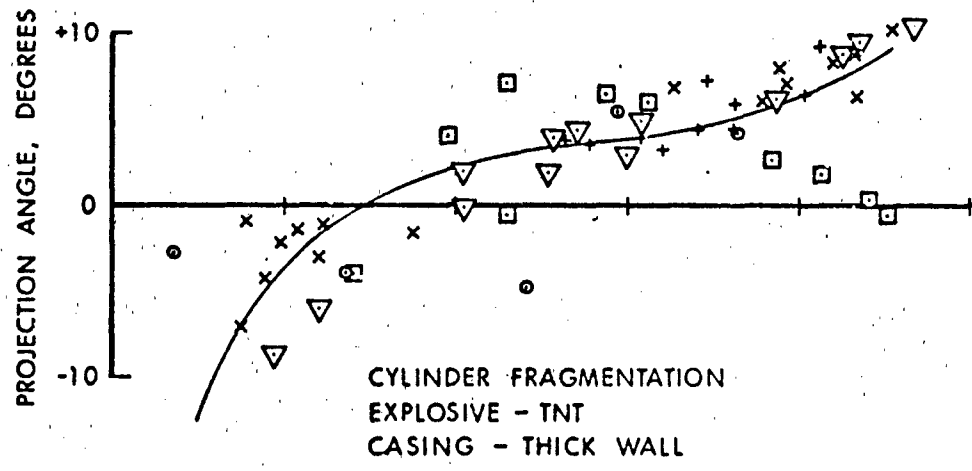
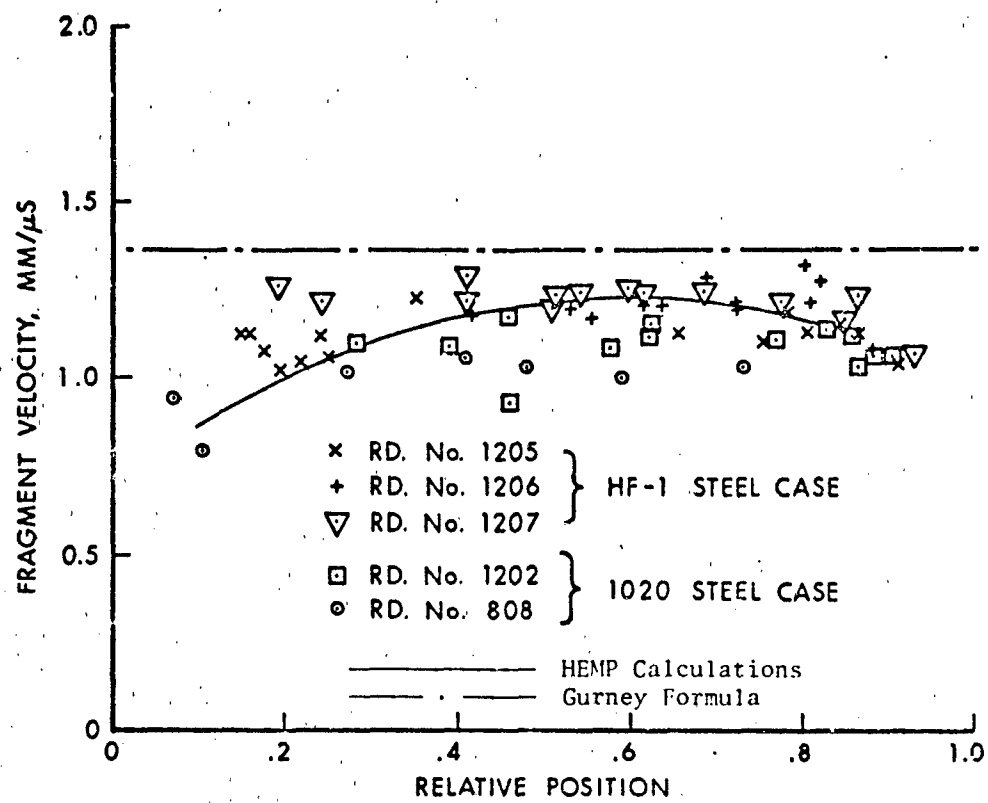


Figure 18. Comparison Between HEMP Calculations and Experimental Data of Fragment Speed and Projection Angle for Cylinders of $L/D = 2$, TNT, $C/M = .4$

105 MM, M1, HE PROJECTILE
 FRAGMENT VELOCITY DISTRIBUTION
 TEST DATA AND CALCULATED RESULTS

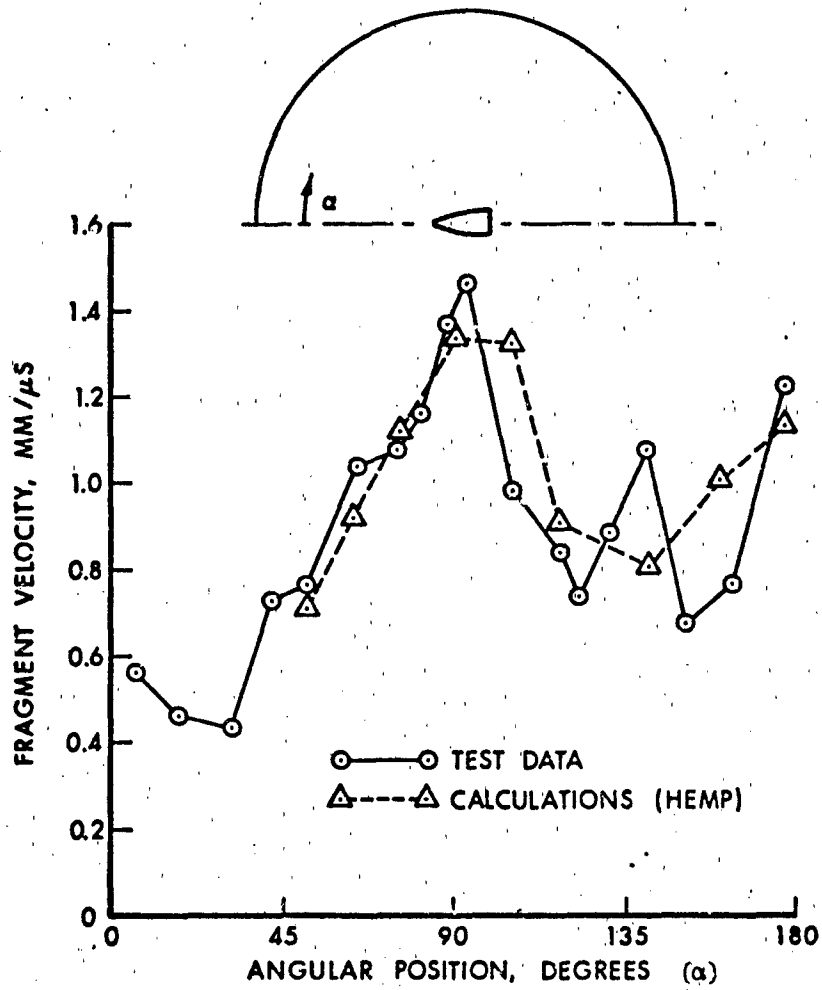


Figure 19. Comparison Between HEMP Calculations and Experimental Data Obtained From Arena Tests - Fragment Speed Versus Angular Position

105 MM, M1, HE PROJECTILE
 FRAGMENT MASS DISTRIBUTION
 TEST DATA AND CALCULATED RESULTS

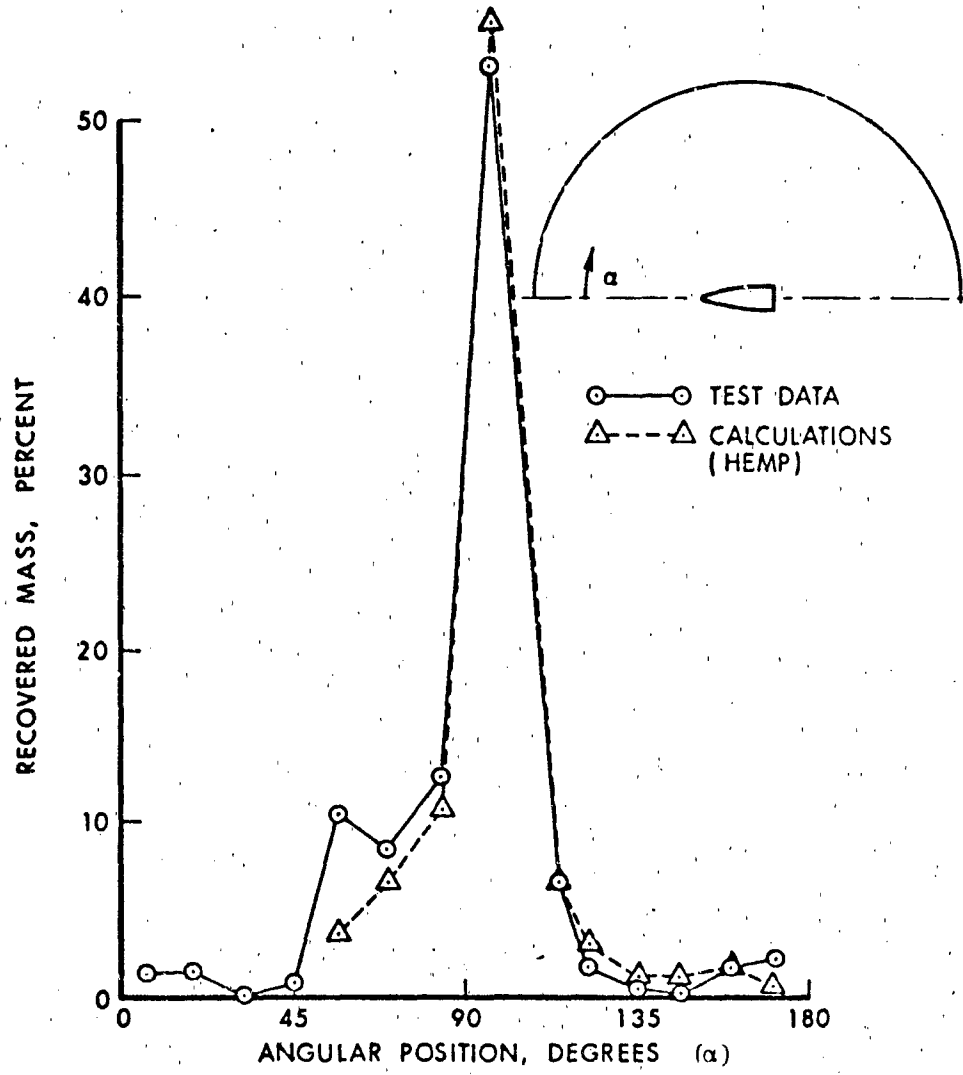


Figure 20. Comparison Between HEMP Calculations and Experimental Data Obtained From Arena Tests - Fragment Mass Versus Angular Position

DISTRIBUTION LIST

| <u>No. of Copies</u> | <u>Organization</u> | <u>No. of Copies</u> | <u>Organization</u> |
|--------------------------|--|--------------------------|---|
| 2 | Commander Defense Documentation Center ATTN: DDC-TCA Cameron Station Alexandria, VA 22314 | 1 | Director US Army Air Mobility Research and Development Laboratory Ames Research Center Moffett Field, CA 94035 |
| 1 | Director of Defense Research & Engineering ATTN: Tech Lib, Rm 3E-1039 Washington, DC 20301 | 1 | Commander US Army Electronics Command ATTN: AMSEL-RD Fort Monmouth, NJ 07703 |
| 2 | Commander US Army Materiel Command ATTN: AMCDMA, N. Klein J. Bender 5001 Eisenhower Avenue Alexandria, VA 22304 | 1 | Commander US Army Missile Command ATTN: AMSMI-R Redstone Arsenal, AL 35809 |
| 1 | Commander US Army Materiel Command ATTN: AMCRD, BG H. A. Griffith 5001 Eisenhower Avenue Alexandria, VA 22304 | 1 | Commander US Army Tank Automotive Command ATTN: AMSTA-RHFL Warren, MI 48090 |
| 1 | Commander US Army Materiel Command ATTN: AMCRD-T 5001 Eisenhower Avenue Alexandria, VA 22304 | 2 | Commander US Army Mobility Equipment Research & Development Center ATTN: Tech Docu Cen, Bldg. 315 AMSME-RZT Fort Belvoir, VA 22060 |
| 1 | Commander US Army Materiel Command ATTN: AMCRD-R 5001 Eisenhower Avenue Alexandria, VA 22304 | 1 | Commander US Army Armament Command Rock Island, IL 61202 |
| 1 | Commander US Army Aviation Systems Command ATTN: AMSAV-E 12th and Spruce Streets St. Louis, MO 63166 | 2 | Commander US Army Picatinny Arsenal ATTN: R. Nixon S. Stein Dover, NJ 07801 |
| | | 5 | Commander US Army Picatinny Arsenal ATTN: SARPA-FR-E Mr. G. Randers-Pehrson Dr. N. Clark Mr. J. Hershkowitz Mr. J. Pearson Tech Lib Dover, NJ 07801 |

DISTRIBUTION LIST

| <u>No. of Copies</u> | <u>Organization</u> | <u>No. of Copies</u> | <u>Organization</u> |
|--------------------------|---|--------------------------|---|
| 4 | Commander US Army Frankford Arsenal ATTN: SARFA-C2500 SARFA-C3200 Mr. P. Gordon Mr. R. Weimer Mr. H. Markus Philadelphia, PA 19137 | 2 | Chief of Naval Research Department of the Navy ATTN: Codes 427, 470 Washington, DC 20325 |
| 1 | Commander US Army Harry Diamond Laboratories ATTN: AMXDO-TI 2800 Powder Mill Road Adelphi, MD 20783 | 3 | Commander US Naval Surface Weapons Center ATTN: Dr. H. Sternberg Dr. M. Kamlet Code 730, Lib Silver Spring, MD 20910 |
| 2 | Commander US Army Materials and Mechanics Research Center ATTN: AMXMR-TF, J. Mescall Tech Lib Watertown, MA 02172 | 2 | Commander US Naval Surface Weapons Center ATTN: Code GWD Tech Lib Dahlgren, VA 22448 |
| 1 | Assistant Secretary of the Army (R&D) ATTN: Asst. for Research Washington, DC 20310 | 1 | Commander US Naval Weapons Center ATTN: Code 45, Tech Lib China Lake, CA 93555 |
| 2 | HQDA (DAMA-ZA; DAMA-AR) Washington, DC 20310 | 1 | Director US Naval Research Laboratory Washington, DC 20350 |
| 1 | Commander US Army Research Office P.O. Box 12211 Research Triangle Park, NC 27709 | 1 | USAF (AFRDDA) Washington, DC 20311 |
| 2 | Commander US Naval Air Systems Command ATTN: Code AIR-310, 350 Washington, DC 20360 | 1 | AFSC (SDW) Adnrews AFB Washington, DC 20311 |
| 1 | Commander US Naval Ordnance Systems Command ATTN; Code ORD-0332 Washington, DC 20360 | 1 | US Air Force Academy ATTN: Code FJS-RL (NC) Tech Lib Colorado Springs, CO 80840 |
| | | 1 | Commander Hill Air Force Base ATTN: Code OOAMA (MMECB) Utah 84401 |
| | | 1 | AFWL (SUL, Lt Tennant) Kirtland AFB, NM 87116 |

DISTRIBUTION LIST

| <u>No. of Copies</u> | <u>Organization</u> | <u>No. of Copies</u> | <u>Organization</u> |
|--------------------------|---|--------------------------|---|
| 1 | AFLC (MMWMC) Wright-Patterson AFB, OH 45433 | 1 | Drexel Institute of Technology Wave Propagation Research Ctr. ATTN: Prof. P. Chou Philadelphia, PA 19104 |
| 1 | AFAL (AVW) Wright-Patterson AFB, OH 45433 | 2 | University of California Los Alamos Scientific Lab. ATTN: Dr. J. Walsh Tech Lib P.O. Box 1663 Los Alamos, NM 87544 |
| 5 | Director Lawrence Livermore Laboratory ATTN: Dr. J. Kury Dr. M. Wilkins Dr. E. Lee Dr. H. Hornig Tech Lib P.O. Box 808 Los Alamos, NM 87544 | | <u>Aberdeen Proving Ground, MD</u> Marine Corps Ln Ofc Dir, USAMSA |
| 1 | Honeywell Inc. Government & Aeronautical Products Division ATTN: C. R. Hargreaves 600 Second Street Hopkins, MN 55343 | | |
| 1 | Physics International Corp. ATTN: Dr. C. Godfrey 2700 Merced Street San Leandro, CA 94577 | | |
| 1 | Sandia Laboratories ATTN: Dr. W. Herrmann P.O. Box 5800 Albuquerque, NM 87115 | | |
| 1 | Shock Hydrodynamics ATTN: Dr. L. Zernow 4710-4716 Vineland Avenue North Hollywood, CA 91602 | | |
| 1 | Systems Science & Software ATTN: Dr. R. Sedgwick P.O. Box 1620 LaJolla, CA 92037 | | |